Cell. Mol. Life Sci.

DOI 10.1007/s00018-006-6126-3

Cellular and Molecular Life Sciences

Research Article

Proteomic analysis of low-abundant integral plasma membrane proteins based on gels

L.-J. Zhang†, X.-e Wang†, X. Peng, Y.-J. Wei, R. Cao, Z. Liu, J.-X. Xiong, X.-f. Yin, C. Ping and S. Liang*

Key Laboratory of Protein Chemistry and Developmental Biology of National Education Committee, College of Life Science, Hunan Normal University, Changsha 410081 (P. R. China), Fax: +86 731 886 1304, e-mail: liangsp@hunnu.edu.cn

Received 15 March 2006; received after revision 17 May 2006; accepted 10 June 2006

Abstract. To characterize low-copy integral membrane proteins and offer some methods for human liver proteome projects, we fractionated highly purified rat liver plasma membrane (PM). PM was purified through two sucrose density gradient centrifugations, and treated with 0.1 M Na_2CO_3, chloroform/methanol and Triton X-100. Proteins were separated by electrophoresis and submitted to mass spectrometry analysis. Four hundred and fifty-seven non-redundant membrane proteins were identified, of which 23% (105) were integral membrane proteins with one or more transmembrane domains. One hundred and fifty-three (33.5%) had no location annotation and 68 were unknown-function proteins. The proteins from different fractions were complementory. A database search for all identified proteins revealed that 53 proteins were involved in the cell communication pathway. More interestingly, more than 50% of the proteins had a protein abundance index concentration of less than 0.1 mol/l, and 12% proteins a concentration 100 times less than that of arginase 1 and actin.

Keywords. Rat liver, plasma membrane, SDS-gel electrophoresis, microdomain.

With the development of human liver proteome projects, the identification of low-copy liver integral membrane proteins has become a major challenge. Large-scale proteomic investigations have more recently turned their focus on subcellular compartments and organelles as more tractable and biologically meaningful targets for comprehensive protein identification [1]. The plasma membrane (PM) is an organized system serving as a structural and communication interface for exchanges of information and substances with the extracellular environment. The membrane proteins on the PM act as 'doorbells' and 'doorways' playing crucial roles in cell function. Integral membrane proteins are important biological and pharmacological targets involved in intercellular communication, cellular development, cell migration, and drug resistance [2–6]. Contemporary genomic analysis indicates that 20–30% of all open reading frames (ORFs) encode integral membrane proteins [7]. However, there is less research on the integral membrane proteome than that of soluble proteins.

A major challenge is the solubility and low abundance of membrane proteins. In classical two-dimensional electrophoresis (2DE), integral membrane proteins tend to be more hydrophobic and they are frequently under-represented primarily due to precipitation of these proteins near their isoelectric points. As a result, one-dimensional electrophoresis (1DE) separations have usually been used to separate membrane protein fractions. In this work, after two sucrose density centrifugations, we obtained a highly purified PM preparation as characterized by Western blot and electron microscopy. The proteins were extracted from the PM using different procedures to retrieve proteins with a wide range of hydrophobicity, i.e., alkaline treatment and chloroform/methanol extraction.

* Corresponding author.
† These authors contributed equally to this work.

Many subcellular fractionation strategies relying on physicochemical methods (e.g. detergent or ultrasonication treatments) have been described as adequate for the isolation of PM microdomains, so their proteomes have been investigated in several recent papers which were reviewed by Raimondo et al. [8]. Such a microdomain strategy has the power to detect microdomain proteins, representing approximately 0.5% of the total cellular protein pool and less than 2% of total PM proteins [9]. Moreover, it should allow comparisons of protein abundance while adding valuable information about localization and function [10]. In this study, the PM was treated with Triton X-100 at 4 °C, and then centrifuged in sucrose. Three main fractions (named fraction 1, 2, and 3) were obtained and fraction 1 was highly enriched in caveolae. Using this method, the low-copy integral membrane proteins were enriched. Mass spectrometric analyses [matrix-assisted laser desorption/ionization (MALDI) time-of-flight (TOF), and electrospray ionization (ESI) tandem mass spectrometry (MS/MS)] were used to identify the PM proteins.

Our present goal was to determine the components of the PM proteins, including those with low abundance and high hydrophobicity. This was achieved by combining subcellular fractionation, microdomain separation, integral membrane enrichment, and protein separation techniques with proteomic-type protein identification. In this study we identified, in the integral plasma membrane protein fractions, 457 non-redundant proteins of rat liver, of which 46% were only from microdomain fractions. Of these, 105 (23%) were integral membrane proteins with one or more transmembrane domains, and 153 (33.5%) have no location annotation. To the best of our knowledge, this is the first systematic investigation of the rat liver low-copy integral plasma membrane proteome.

Materials and methods

Materials. Anti-caveolin monoclonal antibody, anti-sodium potassium ATPase and horseradish peroxidase (HRP)-conjugated anti-mouse IgG were purchased from Upstate (Lake Placid, N.Y.). Anti-flotillin monoclonal antibody was purchased from BD Transduction Laboratories (Lexington, Ky.). Anti-NADH ubiquinol oxidoreductase 39 was from Abcam (Cambridge, UK). LumiGLO chemiluminescent substrate was from KPL (Gaithersburg, Md.). Immobilized pH gradient (IPG) DryStrips (3–10 linear) and IPG buffer were purchased from GE Healthcare (formerly Amersham Biosciences, Uppsala, Sweden). DTT, iodoacetamide, trypsin (proteomics sequencing grade), sodium carbonate, sucrose, Triton X-100, CCA and TFA were obtained from Sigma (St. Louis, Mo.). Acrylamide, bis-acrylamide, urea, glycine, Tris, CHAPS, and SDS were from Amresco (Solon, Ohio). SYPRO RUBY was purchased from Bio-Rad (Hercules, California, USA) PVDF membranes were from Millipore (Bedford, Mass.). Acetonitrile (chromatogram grade) and other chemicals (analytical grade) were from Chinese National Medicine Group Shanghai Chemical Reagent Company. Sprague-Dawley rats (weighting 150 g–200 g, equal number of female and male) were purchased from Hunan Medical University (Changsha, China).

Preparation of rat liver PMs. PMs were purified according to the procedure described in our previous paper followed by a further purification [11]. Briefly, the crude PM (CPM) at the top of 42.3% sucrose was collected and washed. The CPM pellets were transferred to SW-28 tubes, mixed with 50% sucrose, adding homogenization buffer or 50% sucrose to the mixture until the concentration of sucrose was 44%. Then sucrose step gradients containing 42.8%, 42.3%, 41.8%, 41.0%, 39.0%, and 37.0% sucrose were layered on top. The purified PM (PPM) at the top of 37.0% sucrose was collected after centrifugation at 100,000 g for 6 h. Then a specimen of the sample was fixed and analyzed by electron microscopy, the remainder was stored at –80 °C in storage buffer (40 mM HEPES, 1 mM PMSF).

Preparation of integral-enriched membrane fractions using 0.1 M Na_2CO_3. The PPM was treated with 0.1 M Na_2CO_3 according to previous descriptions [12, 13]. PPM stored in storage buffer was diluted 200 times with 0.1 M Na_2CO_3 and kept on ice for 30 min. After centrifugation (15,000 g for 60 min), the pellet was solubilized in lysis buffer containing 4% SDS.

Chloroform/methanol treatment. Cold chloroform/methanol (C/M) (v/v 5 : 4) solution was used to extract integral membrane proteins, as previously described [13]. The mixture was kept on ice for 15 min before centrifugation for 20 min at 12,000 g at 4 °C. The organic phase was dehydrated under nitrogen, cooled and then further dried in a SpeedVac, and solubilized in lysis buffer containing 4% SDS for proteomic analysis.

Preparation of caveolae and raft-enriched membrane fractions using detergent resistance. We employed the well-characterized procedure for caveolae and raft membrane isolation on the basis of resistance to Triton X-100 solubilization at 4 °C and buoyant flotation in sucrose density gradients [10] with some modification. In brief, the PPM was adjusted to 1% Triton X-100 in a Dounce homogenizer at 4 °C by addition of 2% Triton X-100 in PBS, mixed, homogenized by 10 strokes in a glass homogenizer and mixed with 1.5 ml of 50% sucrose, then loaded at the bottom of an SW41 tube (about 3 ml). Five milliliters of 30% sucrose, followed by 4 ml of 5% sucrose was layered on top of the SW41 tube and ultracentrifu-

gation was performed for 18 h at 266,000 g in an SW41 rotor (Beckman Coulter Fullerton, CA, USA) at 4 °C. Three fractions were collected and used for SDS-PAGE analysis followed by immunoblotting. Fraction 1, which was a light-scattering band around the 5–30% interface, was identified as a raft/caveolae-enriched fraction. Two other fractions were also collected and used for low-copy integral membrane proteome analysis. The protein concentration of fractions was measured with RC/DC (Bio-Rad Laboratories, Hercules, California), and they were stored at –80 °C.

Electron microscope analysis of the PM. A specimen of PM was fixed with 2.5% glutaraldehyde overnight at room temperature, washed with ddH_2O twice, fixed with OsO_4 for 2 h, dehydrated with alcohol (sequence of 50%, 70%, 90%, and 100%), followed by dehydration with acetone (50%, and 100%) and processed into epoxy resin. Thin sections (70 nm) were collected on copper grids, stained with uranyl acetate and lead citrate and examined with a JEM-1230 Electron Microscope (JEOL, Tokyo, Japan).

Electrophoresis and Western blotting analysis. Equal volumes (200 µg for proteome analysis and 50 µg for Western blot) of the harvested fractions were separated by 10% SDS-PAGE and stained with Coomassie blue G-250. For immunoblotting, proteins were transferred to PVDF membranes by semidry blotting. Wash buffers were composed of 10 mM Tris, pH 7.5, 150 mM NaCl, 0.1% v/v Tween 20 (TBS-T) supplemented with 5% w/v non-fat dry milk for the blocking solution and the antibody diluents. The membranes were incubated with primary antibodies (diluted with 5% non-fat dry milk according to the protocol of the manufacturers) for 1 h. Then the membranes were washed three times with TBS-T. HRP-conjugated secondary antibodies (1 : 500 dilution) were used in combination with a chemiluminescent substrate to visualize specific signals, according to standard procedures.

Two-dimensional gel electrophoresis. 2DE was performed with the IPGphor system (GE, formerly Amersham Bioscience, Uppsala, Sweden) and PROTEAN II system (BioRad, Hercules, California), as previously described [14]. Briefly, PM proteins (50 µg) were mixed with a rehydration solution containing 8 M urea, 2 M thiourea, 4% CHAPS, 1% NP-40, 20 mM Tris-base, 0.5% (v/v) IPG buffer (pH 3–10), 2 mM TBP and a trace of bromophenol blue to a total volume of 350 µl, and applied to IPG dry strips [pH 3–10 (180 × 30 × 0.5 mm)]. Isoelectricfocusing (IEF) was conduced automatically to a total of 44.1 KVh. After equilibration, proteins were separated in the second dimension on discontinuous SDS-polyacrylamide vertical 1-mm-thick slab gels, with 10–15% separation and 4.8% stacking gels in a Bio-Rad Protein II electrophoresis apparatus. After 2DE, the gels were stained with SYPRO RUBY.

Image acquisition and analysis. The stained gels were scanned using ProxCision (PerkinElmer, Boston, MA, USA). Spot detection was performed using Phoretix 2D software (Nonlinear Dynamics, Newcastle upon Tyne, UK).

In-gel digestion of proteins. The Coomassie blue-stained protein bands and SYPRO RUBY-stained protein spots were excised from gels using a punch and placed into 500-µl Eppendorf tubes. The proteins were digested in-gel with trypsin, as described in our previous work [11, 15]. Briefly, each Coomassie blue-stained band was destained with 50 µl of 50% acetonitrile (ACN) in 25 mM NH_4HCO_3 incubated at 37 °C for 0.5 h, repeated once, followed by washing with H_2O and ACN (proteins from SYPRO RUBY-stained gels were only washed with H_2O and ACN). Then the dried gels were reduced and alkylated. The gel pieces were digested with trypsin (0.02 g/l) in 25 mM NH_4HCO_3 containing 10% ACN at 37 °C overnight. The digested peptides were used for MALDI-TOF-TOF and ESI-Q-TOF analysis.

MALDI-TOF-TOF. The tryptic mixed peptides from 2DE gel spots were loaded onto an AnchorChip™ target plate according to Gobom et al. [16]. Briefly, samples were prepared for analysis by applying 2 µl of digested supernatant material on the surface of a 384 AnchorChip target (Bruker Daltonik, Bremen, Germany) equipped with matrix solution. After incubating for about 3 min, the droplets were washed twice with 2 µl 0.5% TFA to remove contamination from the samples, followed by co-crystallization with 1 µl recrystallization mixture [HCCA (0.1 g/l) in EtOH : acetone : 0.1%TFA, 6 : 3 : 1]. Molecular-weight information of peptides was obtained using a MALDI-TOF-TOF mass spectrometer (UltroFlex I, Bruker Daltonik) equipped with a nitrogen laser (337 nm) and operated in reflector/delay extraction mode for MALDI-TOF-peptide mass fingerprinting (PMF) or LIFT mode for MALDI-TOF-TOF with a fully automated mode using the flexControl™ software. An accelerating voltage of 25 kV was used for PMF. Calibration of the instrument was performed externally with $[M+H]^+$ ions of angiotensin I, angiotensin II, substance P, bombesin, and adrenocorticotropic hormones (clip 1–17 and clip 18–39). Each spectrum was produced by accumulating data from 100 consecutive laser shots, and spectra were interpreted with the aid of the Mascot Software (Matrix Science Ltd, London, UK). The peaks with S/N ≥ 5, resolution ≥ 2500 were selected and used for LIFT-MS/MS from the same target. A maximum of six precursor ions per sample were chosen for MS/MS analysis. In the TOF1 stage, all ions were accelerated to 8 kV under conditions

promoting metastable fragmentation. After selection of a jointly migrating parent and fragment ions in a timed ion gate, the ions were lifted by 19 kV to a high potential energy in the LIFT cell. After further acceleration of the fragment ions in the second ion source, their masses could be analyzed simultaneously in the reflector with high sensitivity. LIFT spectra were interpreted with the Mascot software. Database searches, through Mascot, using combined PMF and MS/MS datasets were performed via BioTools 2.2 software (Bruker), mass tolerance in PMF of 50 ppm, MS/MS tolerance of 1.0 Da and one missing cleavage site and cysteines modified by carbamidomethylation. The protein identifications were considered to be confident when the protein score of the hit exceeded the threshold significance score of 58 ($p < 0.05$). For samples from SDS-PAGE, we basically selected all proteins with probability-based scores (total score) that exceeded its threshold, indicating a significant (or extensive) homology ($p < 0.05$), and referred to as 'hits'. For samples from 2DE, only the first 'hit' protein was selected.

ESI-Q-TOF-MS. The digested samples separated by SDS-PAGE were analyzed by ESI-Q-TOF and Mascot search according to previously described methods [17, 18]. The criteria were based on the manufacturer's definitions (Matrix Science, London, UK) [19]. Proteins identified with at least two peptides showing a score higher than 37 were validated without any manual validation. Those with at least two peptides showing one score higher than 37 and the other higher than 20 and lower than 37 were systematically checked and/or interpreted manually to confirm or cancel the MASCOT suggestion. For proteins identified by only one peptide, its score had to exceed 37, and its peptide sequence was systematically checked manually.

Protein abundance determination. The protein abundance determination was done according to the method described by Liu et al. [20]. To calculate the number of observable peptides per protein, the peptides beyond the scan range of the mass spectrometer (500 3000 Da) were eliminated. All data were calculated manually. For the number of observed peptides per protein, the unique sequences were counted. When the proteins were identified several times, only the peptides in the proteins with highest mass score were counted. All numbers were imported to Excel spreadsheets. The protein abundance index (PAI) is defined as

$$PAI = N_{obsd}/N_{obsbl} \quad \text{(Eq. 1)}$$

where N_{obsd} and N_{obsl} are the number of observed peptides per protein and the number of observable peptides per protein, respectively [20]. The emPAI is defined as

$$emPAI = 10^{PAI} - 1 \quad \text{(Eq. 2)}$$

Thus, the protein contents in molar fraction percentages are described as

$$\text{protein content (mol\%)} = [emPAI/\Sigma(emPAI)] \times 100. \quad \text{(Eq. 3)}$$

Data analysis and bioinformatics. A Perl software was written in-house to pick up significant hits from Mascot output files (html files) into tab-delimited data files suitable for subsequent data analysis. An automated sequence retrieval software was written in Perl using the Bioperl libraries to generate FASTA formatted protein sequence from IPI databases for proteins identified by each MS experiment. The molecular-mass values, pI values and percentage of the protein covered by the matched peptides were retrieved from Mascot output files. The average hydropathy for identified proteins was calculated using the ProtParam software available at http://us.expasy.org by submitting each FASTA file in batch. The proteins exhibiting positive GRAVY values were recognized as hydrophobic and those with negative values were deemed hydrophilic [21]. The subcellular location and function of the identified proteins were elucidated by gene ontology (GO) component and function terms respectively, text based annotation files of which were available for download from the GO database ftp site: ftp://ftp.geneontology.org/pub/go/ [22]. The mapping of putative transmembrane domains in the identified proteins was carried out using the transmembrane hidden Markov model (TMHMM) algorithm, available at http://www.cbs.dtu.dk/services/TMHMM [23].

Results and discussion

Isolation of PM from rat liver tissue. It is important and challenging to obtain enriched PM for the proteomic analysis. We used differential and twofold density gradient centrifugation to isolate PM from fresh rat liver tissue. The quality of the PM was evaluated by electron microscopy and Western blot. Electron microscopy indicated that contamination by mitochondria and other organelles in PPM was much less than in CPM, as shown in Figure 1. PMs were visible as interconnected black lines and the bi-layer membrane structure can be seen at a 50,000-fold magnification (Fig. 1a, b, c, d). In Figure 1a (micrograph of CPM), there are four mitochondria among the PMs. However, only one mitochondrion can be seen in Figure 1c (micrograph of PPM). We further counted mitochondria across ten electron microscope fields for each sample. An average of 3.4 and 1 mitochondria were observed in CPM and PPM, respectively. The preparations were also compared using antibodies against flotillin and Na^+/K^+-ATPase, PM-specific proteins and NADH ubiquinol oxidoreductase 39, a mitochondion-specific protein. As shown in Figure 2a, PPM was about six times

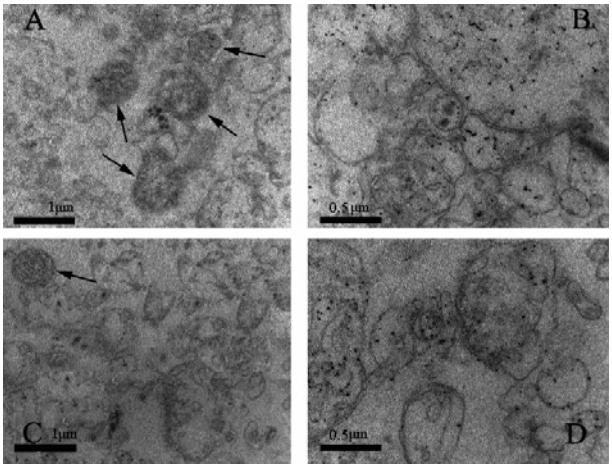

Figure 1. Transmission electron microscope observation of rat liver PM. (*a*) CPM, ×25,000. (*b*) CPM, ×50,000. (*c*) PPM, ×25,000. (*d*), PPM, ×50,000. Arrows indicate the mitochondria among the PM.

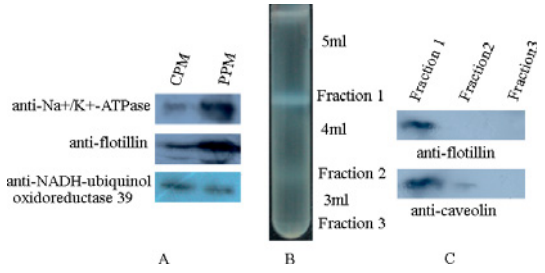

Figure 2. Separation of microdomain fractions and characterization and evaluation of all fractions. (*a*) Detection of organelle-specific proteins in CPM and PPM by Western blot. Fifty micrograms of CPM and PPM proteins were separated in 10% SDS-PAGE and transferred to a PVDF membrane. The blots were probed with antibodies against organelle-specific proteins: anti-Na^+/K^+-ATPase and anti-flotillin for PM; anti-NADH-ubiquinol oxidoreductase 39 for mitochondria. (*b*) Microdomain fraction separation by sucrose density centrifugation; three fractions named fraction 1, 2, and 3 were obtained. (*c*) Western blot of microdomain fractions. Fraction 1 contains caveolin- and flotillin-enriched caveolae.

purer than CPM judged by the PM-specific antibodies, and the contaminants were decreased 1.5-fold as judged by mitochondria antibodies through Quantity One 4.1.0 (Bio-Rad) software analysis. These data confirm the high degree of enrichment of the PM fraction and its low level of contamination by other organelles. Microdomains obtained after Triton X-100 treatment and a discontinuous sucrose gradient centrifugation were named fraction 1 (light band), fraction 2 (heavy band) and fraction 3 (pellets) (Fig. 2b). Fraction 1 showed a higher concentration of caveolin and flotillin than fractions 2 and 3 which showed almost no caveolin and flotillin signals (Fig. 2c). So, fraction 1 contained caveolin-enriched domains, from which proteins were extracted, separated by 2DE and SDS-PAGE. Protein fractions 2 and 3 were separated by SDS-PAGE. All separated proteins were submitted to mass spectrometry analysis.

Enrichment and separation of low-abundant integral membrane proteins. A survey of the literature shows that hydrophilic proteins are routinely extracted by non-ionic detergents like Triton X-100 or by alkaline treatments such as Na_2CO_3, and hydrophobic proteins are recovered in the pellet after centrifugation [24, 25]. Organic solvents such as C/M have been used successfully for solubilizing highly hydrophobic proteins from membranes of the chloroplast envelope [26], thylakoids [27] and PM [25]. The C/M ratio 5 : 4 (v/v) was found optimal for a hydrophobic protein solution. Thus, in this research, hydrophobic proteins were extracted with a C/M ratio of 5 : 4 (v/v) or with lysis buffer containing 4% SDS after treatment of Na_2CO_3. Furthermore, low-abundant proteins were usually beyond the scope of standard proteomic techniques for the overlap of abundant proteins. For the removal of abundant proteins and enrichment of low-abundant proteins, two methods are possible: (1) sequential extraction; (2) fractionation. Here, we first used a fractionation strategy to separate PM into three fractions and identified each fraction. Whatever the method used, proteins were then submitted to SDS-PAGE analyses, except those from fraction 1 highly enriched in caveolae, which was also separated with 2DE (pH 3–10) (Fig. 3). The electrophoresis profiles were very different in these fractions from those of the total PM proteins. Many low-molecular-weight protein bands were removed, and new high-molecular-weight protein bands were especially apparent in the C/M extracts. Protein bands from fractions 1, 2, and 3 were also different from each other, and complemented each other, as shown in Figure 4a. To understand how many proteins can be represented in 2DE gels

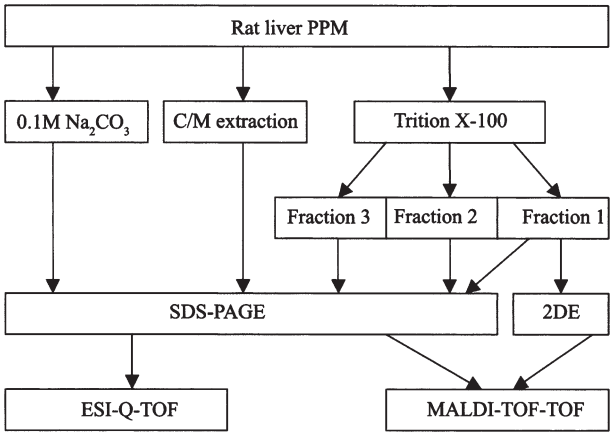

Figure 3. Strategies for protein separation and MS analysis. The purified PM was treated with 0.1 M Na_2CO_3, C/M extraction, and Triton X-100. After Triton X-100 treatment and a discontinuous sucrose gradient centrifugation, PM was separated into three fractions (1, 2, and 3). Fraction 1 was separated by SDS-PAGE and 2DE, the others were separated by SDS-PAGE. Proteins separated by SDS-PAGE were in-gel digested and submitted to ESI-Q-TOF and MALDI-TOF-TOF analysis. Proteins separated by 2DE were only analyzed by MALDI-TOF-TOF.

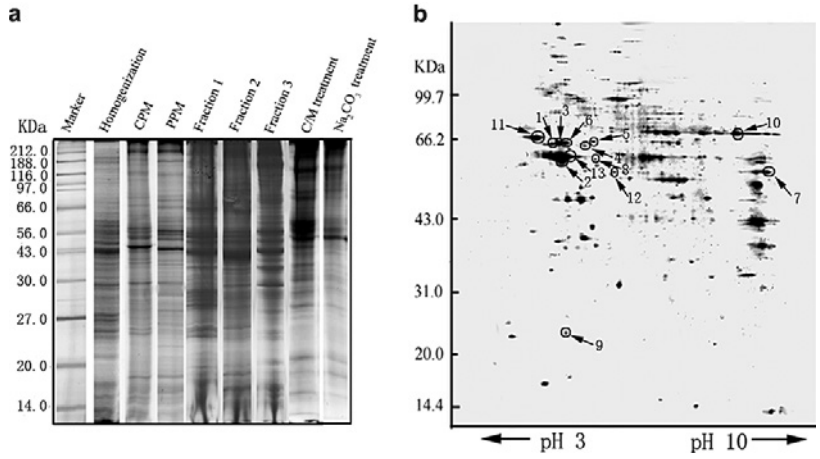

Figure 4. The separation of proteins from fractions by SDS-PAGE and 2DE. (*a*) SDS-PAGE, 200 µg protein was loaded and stained with G-250. (*b*) 2DE, pH 3–10, 50 µg protein was loaded and stained with SYPRO RUBY.

from a caveolae-enriched fraction, proteins from fraction 1 were separated by a pH 3–10 gel. About 300 spots were observed (Fig. 4b).

Proteins identified in rat liver PM. The MS or MS/MS spectra acquired were matched by searching the International Protein Index (IPI) protein sequence database. To avoid false-positive hits, we first used data only from the rat database to avoid a low confidence identification of a non-specific database. Second, we applied stricter criteria for peptide identification than those in most reports [28, 29]. Third, we manually checked the mass spectra of the identified peptides using different filters. A total of 457 non-redundant proteins were identified (see Supplementary Table 1 at http://protchem.hunnu.edu.cn). Although some proteins were identified by only a single peptide, 83% of the proteins contributed by ESI-Q-TOF listed in the supplement were identified by two or more peptides at the 95% confidence level ($p < 0.05$); for proteins identified by MALDI-TOF-TOF, only 8 proteins were identified by PMF, the others had one or more peptides analyzed by LIFT. Among the identified proteins, 197 were from the 0.1 M Na_2CO_3 treatment strategy and 80 from the C/M extraction strategy. The microdomain fractions after treatment with Triton X-100 contained 290. The three methods shared 23 proteins. There were 77 proteins from the microdomain strategy and 0.1 M Na_2CO_3, and only 29 from 0.1 M Na_2CO_3 and C/M (Fig. 5a). Among the identified 290 proteins, there were 93 from fraction 1, 110 from fraction 2, and 201 from fraction 3. Of all identified proteins from fraction 1, 20 were separated with 2DE. There were only 32 proteins (corresponding to 11%) found in all three fractions. Most of the proteins showed a domain-specific pattern, as indicated by the detection of 42, 38 and 128 proteins only from fraction 1, 2, and 3, respectively (Fig. 5b). Thus, these methods are complementary and favor the identification of low-abundance integral membrane proteins.

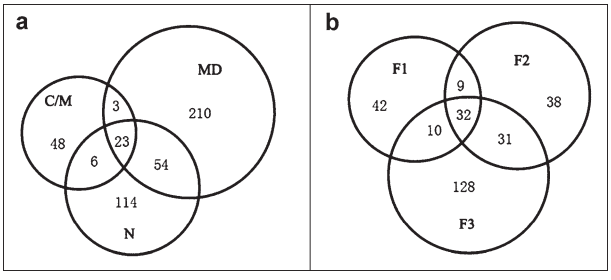

Figure 5. Distribution of proteins identified in different fractions. (*a*) Different treatments. N, Na_2CO_3 treatment; MD, microdomain strategy; C/M, chloroform/methanol extraction. (*b*) Different fractions from the microdomain strategy. F1, F2, and F3 represent fraction 1, 2, and 3 respectively.

Quantitation using emPAI. We used emPAI to estimate the abundance of the proteins (Eqs. 1, 2). To calculate the absolute mol concentrations, the total protein amounts were measured as by SUM assay, and the mol fractions of 431 proteins only, identified by ESI-Q-TOF, were calculated using Equation 3. As shown in supplementary Table 1, 212 proteins have an emPAI less than 0.19, and emPAI-based concentrations less than 0.1 mol/l of the 50 proteins with the lowest concentration analyzed, 37 were from the microdomain strategy, 9 from the Na_2CO_3 treatment, and 6 from the C/M strategy.

To validate the method efficiency, the proteins identified in fraction 1 by both methods were analyzed. The results showed that the emPAI values calculated from the ESI-Q-TOF data were coincident with the quantities observed in the 2DE (Fig. 4b and supplementary Table 1).

Analysis of identified proteins. Several physicochemical characteristics of the 457 identified proteins were analyzed according to their molecular weight (MW),

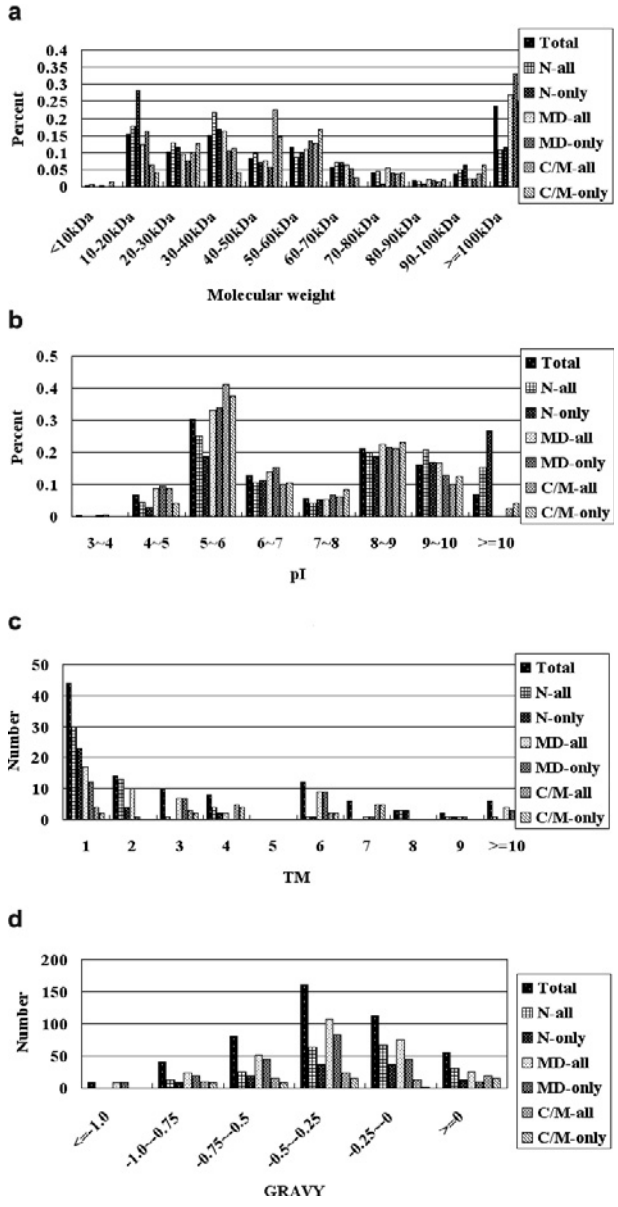

Figure 6. The physicochemical characteristics of the 457 identified proteins including the molecular mass (*a*), pI (*b*), the number of transmembrane domains (TM) (*c*) and hydrophobicity (GRAVY value) (*d*) in different treatments. Total, all proteins identified in this study; N-all, all proteins identified by the Na_2CO_3 strategy; N-only, proteins identified only by the Na_2CO_3 strategy; MD-all, all proteins identified by the microdomain strategy; MD-only, proteins identified only by the microdomain strategy; C/M-all, all proteins identified by C/M extraction; C/M-only, proteins identified only by C/M extraction.

pI, hydrophobicity (GRAVY value), and the number of transmembrane domains (TMs) (Fig. 6).

In the present work, more proteins with a molecular mass above 100 kDa and below 10 kDa were observed in SDS-PAGE than in the 2DE of fraction 1. For all the identified proteins, the smallest and the largest molecular mass were 8.7 and 1849 kDa, respectively. Among the 457 identified proteins, there were 108 (23.6%) proteins with a mass >100 kDa, higher than our previous total PM proteomic analysis [11, 18]. The data in Figure 6a and Table 1 indicate that the C/M extraction strategy and the microdomain pre-fractionation strategy were better than the Na_2CO_3 treatment in the identification of proteins with a high molecular weight, especially in the identification of proteins with mass >100 kDa. The upper ten proteins with a MW >500 kDa were all from the microdomain fractions, except two from C/M: predicted: titin (MW: 1,849,637), predicted: similar to bullous pemphigoid (MW: 1,263,992). Furthermore, all ten proteins were at low concentration. The reason might be that these proteins with low abundance cannot be detected in total integral PM. This result shows the efficiency of our microdomain pre-fractionation strategy in enriching the high-MW proteins. For low-molecular-weight proteins, none of our strategies show superiority, especially for those below 10 kDa. Different electrophoresis systems such as Tricine SDS-PAGE might be a choice for these interesting proteins [30].

The pI distribution, ranging from 3.87 to 11.54, was bimodal, located mainly in the ranges pH 5~6 and 8.0~10 (Fig. 6b). A total of 424 proteins (92.8%) were in the range pI 4–10 but 21 (4.6%) had a pI < 4.3, and 32 (7.0%), a pI > 10, beyond the 2DE separation capability [31]. As shown in Figure 6b and Table 1, proteins with pI > 10 were found only in the fractions extracted with Na_2CO_3 and C/M. In the top ten proteins with high pI, nine were from the Na_2CO_3 treatment and one from C/M. Alkaline Na_2CO_3 may dissolve acidic proteins better, resulting in the enrichment of alkaline proteins. However, the weakly acidic C/M solution and neutral Triton X-100 have weaker extraction or enrichment power than alkaline Na_2CO_3 for high pI proteins. For the ten proteins with low pI, no strategy was found to dominate. Thus, Na_2CO_3 treatment is better suited for alkaline integral membrane proteome research.

Of the total 457 proteins, 105 (23%) have one or more theoretical TM domains predicted by TMHMM, and 46 (58%) of the TM-spanning proteins contain two or more TM domains (Fig. 6c). The microdomain fractionation strategy was better than the C/M and Na_2CO_3 strategies in obtaining proteins with high TM regions, giving four proteins with more than ten TM regions, while C/M and Na_2CO_3 treatment gave two and one protein(s) respectively (Table 1). This may be due to the enrichment of low-abundant highly hydrophobic proteins in the microdomain fractionation strategy. The concentrations based on emPAI verified our hypotheses: all ten proteins were at low concentration (Supplementary Table 1 and Table 1).

The percentage of proteins with TM regions was not very high in this work. This may be due to limitations imposed by the criterion of the presence of putative α helices. (i) Proteins of the porin-type, known to form a β barrel embedded in the membrane lipid bilayer, have no α helix and are therefore not predicted as TM proteins. For example,

Table 1. Proteins with special physicochemical characteristics.

Accession number	Protein name	MW	pI	GRAVY [1]	TM [2]	Source [3]	emPAI	Concentration [4]
			Proteins with molecular weight in the top 10					
IPI00358011	Predicted: dynein, axonemal, heavy polypeptide 1	519025	8.81	–0.266	0	C/M	0.024	0.012
IPI00230794	splice isoform 4 of plectin 1	519746	5.61	–0.689	0	F2,F3	0.147	0.077
IPI00569024	plectin 10	520045	5.6	–0.688	0	F2,F3	0.147	0.077
IPI00559406	plectin 1	521460	5.59	–0.693	0	F2,F3	0.148	0.077
IPI00454444	splice isoform 1 of plectin 1	535152	5.71	–0.681	0	F2,F3	0.144	0.075
IPI00209000	plectin 6	535379	5.71	–0.685	0	F2,F3	0.144	0.075
IPI00565567	534-kDa protein	535418	5.7	–0.683	0	F2,F3	0.145	0.076
IPI00388754	Predicted: similar to N2B-titin Isoform	791896	8.98	–0.477	0	C/M	0.014	0.007
IPI00362153	Predicted: similar to bullous pemphigoid antigen 1-b	1263992	5.56	–0.597	0	F3	0.006	0.003
IPI00373635	Predicted: titin	1849637	5.56	–0.504	0	F2	0.004	0.002
			Proteins with pI in the top 10					
IPI00231974	histone H2A, testis	14144	11.02	–0.465	0	N	2.728	1.426
IPI00566442	Predicted: similar to histone H2A.1	15305	11.02	–0.484	0	N	1.783	0.932
IPI00200624	14-kDa protein	14037	11.05	–0.405	0	N	2.728	1.426
IPI00560491	Predicted: similar to histone H2A.l (H2A/l)	14111	11.05	–0.458	0	N	2.728	1.426
IPI00214497	H2A histone	14167	11.05	–0.487	0	N	2.728	1.426
IPI00476506	24-kDa protein	24170	11.36	–0.835	0	N	0.122	0.064
IPI00393399	24-kDa protein	24303	11.42	–0.826	0	N	0.122	0.064
IPI00390829	Predicted: similar to 60S ribosomal protein L13	24079	11.47	–0.842	0	N	0.116	0.061
IPI00230916	60S ribosomal protein L13	24221	11.54	–0.908	0	N	0.129	0.067
IPI00206037	Predicted: secretory carrier membrane protein 3	38743	11.54	0.042	4	C/M	0.233	0.122
			Proteins with pI in the bottom 10					
IPI00192336	proliferation-related acidic leucine-rich protein PAL31	31216	3.87	–1.259	0	F3	0.931	0.487
IPI00569803	Predicted: similar to myosin regulatory light chain-like	15324	4.28	–0.691	0	F1	0.668	0.349
IPI00561918	9-kDa protein	8759	4.45	–0.264	0	F1,F2,F3,N,C/M	1.512	0.791
IPI00567242	17-kDa protein	17124	4.46	–0.403	0	N	0.212	0.111
IPI00392935	17-kDa protein	16962	4.56	–0.404	0	N	0.212	0.111
IPI00209019	rat protein kinase C family-related	27005	4.57	–0.235	0	F2	0.233	0.122
IPI00209908	cytochrome c oxidase subunit 2	26099	4.6	0.269	2	F1,N	3.462	1.904
IPI00607205	Predicted: hypothetical protein XP_579508	100070	4.61	–0.337	1	F1	0.199	0.104
IPI00362131	neural-cadherin precursor	100088	4.61	–0.347	1	F1	0.199	0.104
IPI00561235	cadherin 2	100214	4.63	–0.35	1	F1	0.205	0.107
			Proteins with GRAVY in the bottom 10					
IPI00192336	proliferation-related acidic leucine-rich protein PAL31	31216	3.87	–1.259	0	F3	0.931	0.487
IPI00569214	66-kDa protein	66411	5.16	–1.1	0	F2	0.051	0.027
IPI00214905	tropomyosin alpha 4 chain	28419	4.66	–1.068	0	F3	0.269	0.141
IPI00191354	33-kDa protein	33361	4.73	–1.062	0	F2	0.218	0.114
IPI00372259	tropomyosin	29221	4.75	–1.027	0	F2	0.280	0.146

Table 1. (Continued).

Accession number	Protein name	MW	pI	GRAVY [1]	TM [2]	Source [3]	emPAI	Concentration [4]
IPI00567369	tropomyosin isoform 6	29249	4.75	–1.018	0	F2	0.280	0.146
IPI00324444	putative transcription factor LUZP	120252	8.24	–1.015	0	F2	0.027	0.014
IPI00559772	58-kDa protein	60402	9.45	–1.008	0	F1	0.044	0.023
IPI00558688	Predicted: similar to ribosomal protein L13	12047	9.88	–0.978	0	N	0.259	0.135
IPI00200118	91-kDa protein	91403	5.13	–0.978	0	F2	0.071	0.037
Proteins with GRAVY in the top 10								
IPI00561480	53-kDa protein	53808	9.31	0.303	6	N	0.172	0.090
IPI00187967	Predicted: hypothetical protein XP_217094	21456	8.73	0.341	4	C/M	0.931	0.487
IPI00206080	transmembrane 7 superfamily member 2	46700	5.74	0.474	7	C/M	0.166	0.087
IPI00196643	solute carrier family 2, facilitated glucose transporter, member 2	57448	8	0.505	11	C/M	0.166	0.087
IPI00561686	43-kDa protein	43562	5.57	0.559	6	C/M	0.212	0.111
IPI00208940	claudin-3	23869	7.15	0.605	4	C/M	1.512	0.791
IPI00562709	Cd81 protein	26571	6.9	0.663	4	C/M	0.668	0.349
IPI00188509	defender against cell death 1	12529	4.75	0.815	3	C/M	0.468	0.245
IPI00198900	MAL2A	19473	6	0.833	4	N	2.162	1.131
IPI00464615	tumor suppressing subtransferable candidate 5	44245	5.39	0.931	10	C/M	0.212	0.011
Proteins with TM in the top 10								
IPI00231451	sodium/potassium-transporting ATPase alpha-3 chain	113070	5.26	–0.007	8	N	0.044	0.023
IPI00205693	sodium/potassium-transporting ATPase alpha-2 chain precursor	113480	5.39	–0.007	8	N	0.037	0.019
IPI00195615	bile salt export pump	147267	7.1	0.045	9	N	0.029	0.015
IPI00388475	97-kDa protein	98402	6.75	0.139	9	F3	0.029	0.015
IPI00326305	sodium/potassium-transporting ATPase alpha-1 chain precursor	114316	5.3	0.002	10	F1,F2,N	0.126	0.066
IPI00464615	tumor suppressing subtransferable candidate 5	44245	5.39	0.931	10	C/M	0.212	0.111
IPI00203637	anion exchange protein 4	106412	6.53	0.207	11	F3	0.212	0.111
IPI00196643	solute carrier family 2, facilitated glucose transporter, member 2	57448	8	0.505	11	C/M	0.166	0.087
IPI00199192	voltage-dependent T-type calcium channel alpha-1G subunit	253611	6.99	–0.131	17	F2	0.042	0.022
IPI00339110	254-kDa protein	257364	6.76	–0.132	18	F2	0.042	0.022

[1] Grand average of hydrophobicity.
[2] Predicted number of transmembrane α helices returned by TMHMM. (http://www.cbs.dtu.dk/services/TMHMM).
[3] C/M, N, F1, F2, F3 represent C/M extraction, Na_2CO_3 treatment, fraction 1, fraction 2, and fraction 3, respectively.
[4] emPAI-based mol concentrations.

our method revealed the presence of different voltage-gated channels and their associated proteins (Supplementary Table 1), such as voltage-gated sodium channel subunit β1-A, voltage-dependent anion-selective channel protein 2, voltage-dependent anion-selective channel protein 1, and voltage-gated sodium channel subunit β1-A. (ii) Some of the proteins lacking putative α helices can be predicted to be anchored to the membrane owing to hydrophobic tails and post-translational modifications, such as myristoylation and prenylation. Of course, many integral membrane proteins that are more hydrophobic, especially those with multiple TM domains, have fewer tryptic cleavage sites (hydrophilic residues R and K) and are frequently glycosylated, which may prevent access

of the protease, hence reduce the number of identifiable tryptic peptides, which escape correct identification by mass spectrometry.

The hydrophobic property of proteins is frequently expressed as the GRAVY, index. Proteins detected in 2D-PAGE gels are generally hydrophilic [32, 33]. For the 457 proteins we identified, their GRAVY values varied in the range of –1.259 to 0.931 (Fig. 6d). Only 40 (12%) proteins have positive values. The majority of the analyzed proteins (56.2%) have a GRAVY between +0.4 and –0.4, which could not discriminate their hydrophobic or hydrophilic nature [13, 24]. For example, on the one hand, the 254-kDa protein (IPI00339110), which was characterized by microdomain strategies, displaying 18 TM domains and generally considered to be a highly hydrophobic protein, has a negative GRAVY while the sodium/potassium-transporting ATPase α-1 chain precursor (IPI00326305) with 10 TM regions has a GRAVY of only 0.002 and 3-hydroxyacyl-CoA dehydrogenase type II (IPI00231253) and predicted: similar to prohibitin (IPI00370387) without a predicted TM domain has a GRAVY of more than 0.1. Our data for the PM proteome showed slightly fewer TM proteins than several published reports [34–36], possibly due to using a partly 2DE strategy instead of a shotgun strategy. We found that the top ten proteins with a high GRAVY were all from the C/M strategy except two which came from the Na_2CO_3 treatment. However, the ten proteins with the lowest GRAVY were all from the microdomain strategy, bar 1 from the Na_2CO_3 treatment (Table 1). Interestingly, the ten proteins with the lowest GRAVY were all at a low concentration (less than 0.15) except one with a higher concentration of 0.487, while the ten proteins with the highest GRAVY had a wide concentration range. These results show that C/M is the best method for the extraction of hydrophobic integral membrane proteins, but not low-abundance proteins; the microdomain strategy is the best for the low-abundance analysis, but not for hydrophobic proteins.

The subcelluar locations of the identified proteins were categorized according to the universal GO cellular component annotation. Three hundred and four (66.5%) proteins had a GO annotation for cell-component or cellular locations, of which 190 (62.5%) were PM or PM-related proteins. The remainder were localized primarily to unknown places (33%), the mitochondrion (10.0%), nucleus (7%), and cytoplasm (5%) as shown in Figure 7a. Among the 190 identified PM proteins, 13 are associated with intermediate filaments and 34 with the cytoskeleton. That mitochondrial, nuclear, and cytoplasmic proteins were also identified may be due to other organelles in close contact with the PM, or to the existence of proteins at more than one site in the cell. Of course, some are true contamination proteins because the purification was less than 100% perfect. It is not unusual for proteins initially categorized as organelle specific to be discovered later elsewhere in the cell. For example, histones are able to cross cell PMs and mediate penetration of macromolecules covalently attached to them [37–39]. However, in our study, the histones were categorized in the nucleus according to the GO cellular component annotation, which may be one of the main reasons why we detected so many nuclear proteins (7%). It is often difficult to conclude whether these 'contaminants' represent true endogenous partners or artificial associations induced by cell disruption or incomplete purification. Recently, a comparative proteomics strategy was applied to analyze the relative levels of proteins in different organelle-enriched fractions. This can solve the problem of contaminants and distinguish between proteins from different subcellular compartments without the need to obtain pure organelles [40]. It seems important to look for a useful approach to confirm the location of the PM proteins.

Lastly, we categorized the identified proteins according to their reported function. Three hundred and eighty-nine (85.1%) identified proteins have a GO function description. Of 457 non-redundant proteins, 35% and 29% are proteins with binding and catalytic activity, respectively. Nine percent are involved in cell structure and 8% have transporter activity. Other annotated proteins have special activities such as signal transducer activity, motor activity, antioxidant activity and so on, as shown in Figure 7b. The two most abundant classes of proteins were classified as being involved in binding and catalytic activity,

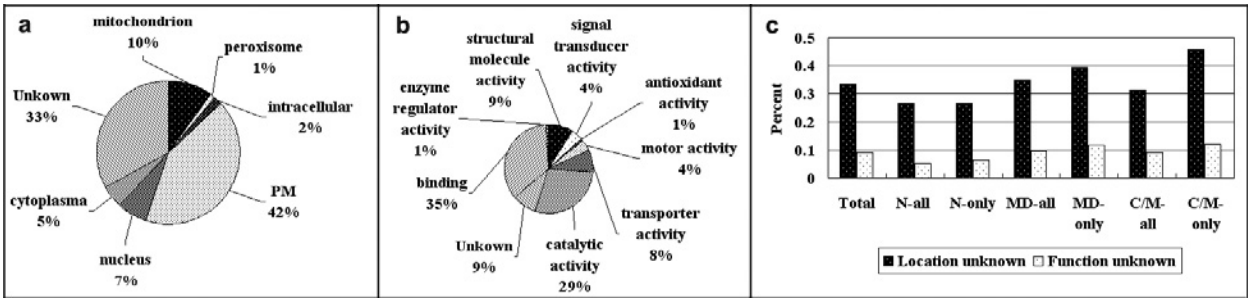

Figure 7. (*a*) The location of proteins identified according to the GO annotation. (*b*) The function distribution of identified proteins. (*c*) the percent of unknown proteins identified in different strategies.

Table 2. Proteins involved in the cell communication pathway.

Accession	Protein name	Source [1]
	Focal adhesion	
IPI00209019	rat protein kinase C-family related	F2
IPI00213463	alpha-actinin 4	F1
IPI00421625	myosin regulatory light chain	F1
IPI00551592	myosin regulatory light chain 2-A, smooth muscle isoform	F1
IPI00367479	Predicted: similar to non-muscle myosin II-C heavy chain	F1,F2,F3, N
IPI00564409	Predicted: similar to myosin regulatory light chain 2-A, smooth muscle isoform (myosin)	F1
IPI00569803	Predicted: similar to myosin regulatory light chain-like	F1
IPI00358406	catenin (cadherin-associated protein), alpha 1, 102 kDa	F1,F2
	Adherens junctin	
IPI00200757	splice isoform 1 of fibronectin precursor	F3
IPI00231982	splice isoform 2 of fibronectin precursor	F3
IPI00231983	splice isoform 3 of fibronectin precursor	F3
IPI00231984	splice isoform 4 of fibronectin precursor	F3
IPI00358406	Catenin (cadherin-associated protein), alpha 1, 102 kDa	F1,F2
IPI00362131	neural-cadherin precursor	F1
IPI00561235	cadherin 2	F1
IPI00370681	capping protein (actin filament) muscle Z-line, alpha 2	N,C/M
IPI00454431	brain-specific alpha actinin 1 isoform	F1
IPI00559362	alpha actinin	F1
IPI00213463	alpha-actinin 4	F1
IPI00563379	actin, cytoplasmic 2	F1,F2,F3, N,C/M
IPI00194087	actin, alpha cardiac	F1,F2,F3, N,C/M
IPI00197129	actin, aortic smooth muscle	F1,F2,F3, N,C/M
IPI00358046	Predicted: similar to actin related protein 2/3 complex subunit 2	F2,F3
IPI00209082	alpha-actinin 1	F1
IPI00189813	actin, alpha skeletal muscle	F1,F2,F3, N,C/M
IPI00200455	actin, gamma-enteric smooth muscle	F1,F2,F3, N,C/M
IPI00363828	Predicted: ARP3 actin-related protein 3 homolog	F3
IPI00189819	actin, cytoplasmic 1	F1,F2,F3, N,C/M
IPI00388662	Predicted: similar to transient receptor potential phospholipase C-interacting kinase	F3
IPI00203398	Predicted: similar to polymerase delta-interacting protein 38	F1
IPI00207550	Predicted: similar to actin, cytoplasmic 2 (gamma-actin)	F1,F2,F3, N,C/M
IPI00358127	Predicted: similar to actin-related protein 3-beta	F3
IPI00559007	Predicted: similar to actin 3-fruit fly (*Drosophila melanogaster*) (fragments)	F1,F2,F3, N
IPI00363867	Predicted: similar to putative type 5 non-muscle actin	F1,F2,F3, N,C/M
IPI00208940	claudin-3	C/M
	gap junction	
IPI00193425	splice isoform 2 of basigin precursor	N
IPI00382166	splice isoform 1 of basigin precursor	N
IPI00209764	glomerular mesangial cell receptor protein-tyrosine phosphatase precursor	F3
IPI00327518	arginase 1	F1,F2,F3,N,C/M
IPI00566583	malate dehydrogenase, mitochondrial	F1,F2,F3
IPI00556929	splice isoform 1 of voltage-dependent anion-selective channel protein 3	N
IPI00370681	capping protein (actin filament) muscle Z-line, alpha 2	N,C/M
IPI00203398	Predicted: similar to polymerase delta-interacting protein 38	F1
IPI00231134	guanine nucleotide-binding protein beta subunit 2-like 1	F3
IPI00564245	Predicted: similar to glutamate receptor, ionotropic, N-methyl D-aspartate-like 1A	C/M

Table 2. (Continued).

Accession	Protein name	Source [1]
	Tight junction	
IPI00454431	brain-specific alpha actinin 1 isoform	F1
IPI00209082	alpha-actinin 1	F1
IPI00200067	junctional adhesion molecule, JAM	F1,
IPI00209019	rat protein kinase C family related	F2
IPI00563379	actin, cytoplasmic 2	F1,F2,F3,N,C/M
IPI00194087	actin, alpha cardiac	F1,F2,F3,N,C/M
IPI00197129	actin, aortic smooth muscle	F1,F2,F3,N,C/M
IPI00559362	alpha actinin	F1
IPI00213463	alpha-actinin 4	F1
IPI00208315	Predicted: similar to myosin-VIIb	F1,F2,F3,N,C/M
IPI00211813	neuronal myosin heavy chain	F1,F2,F3,N,C/M
IPI00209113	myosin heavy chain, non-muscle type A	F1,F2,F3,N,C/M
IPI00421625	myosin regulatory light chain	F1
IPI00551592	myosin regulatory light chain 2-A, smooth muscle isoform	F1
IPI00607166	Predicted: similar to Myh11 protein	F2
IPI00564409	Predicted: similar to myosin regulatory light chain 2-A, smooth muscle isoform	F1
IPI00569803	Predicted: similar to myosin regulatory light chain-like	F1
IPI00358406	catenin (cadherin-associated protein), alpha 1, 102 kDa	F1,F2
	ECM-receptor interaction	
IPI00360737	Predicted: similar to alpha 3 type VI collagen isoform 1 precursor	F3
IPI00371853	Predicted: similar to collagen alpha1 type VI-precursor	F1,F3
IPI00372839	Predicted: similar to alpha 2 type VI collagen isoform 2C2a precursor	F3,N
IPI00200757	splice isoform 1 of fibronectin precursor	F3
IPI00231982	splice isoform 2 of fibronectin precursor	F3
IPI00231983	splice isoform 3 of fibronectin precursor	F3
IPI00231984	splice isoform 4 of fibronectin precursor	F3
IPI00209258	spectrin alpha chain, brain	C/M
	Wnt signaling pathway	
IPI00388662	Predicted: similar to transient receptor potential phospholipase C-interacting kinase	F3
	TGF-beta signaling pathway	
IPI00324444	putative transcription factor LUZP	F2
	Neuroactive ligand-receptor interaction	
IPI00564245	Predicted: similar to glutamate receptor, ionotropic, N-methyl D-aspartate-like 1A	C/M

[1] C/M, N, F1, F2, F3 represent C/M extraction, Na_2CO_3 treatment, fraction 1, fraction 2, and fraction 3 respectively.

which is in accordance with the functional distribution of PM proteins.

Furthermore, comparing the unknown proteins from different strategies, we found that C/M and microdomain strategies identified more proteins with unknown function and location than the Na_2CO_3 strategy (shown in Fig. 7c). This might have been due to the extraction capacity of C/M for hydrophobic membrane proteins and the enrichment in the microdomain strategy of low-abundance proteins.

To judge the efficacy of a global proteomic analysis, we analyzed proteins involved in the cell communication pathway according http://www.genome.ad.jp/kegg/. Fifty-three non-redundant proteins were identified as being involved in cell communication, including adhesion, receptors and so on (Table 2, Fig. 8) [41]. Nineteen proteins were found to be involved in tight junction communication in this work, such as junctional adhesion molecule (JAM), Rat protein kinase C family related, α-actinin 1, 4 and so on, which interact in a network from JAM, ZO-1, α-catenin, actin, to PKC (Table 2, Fig. 8). Twenty-six adherens-junction-related proteins were identified, including fibronectin 1, 2, 3, and 4, catenin, cadherin 2, neural-cadherin precursor, and actin, which

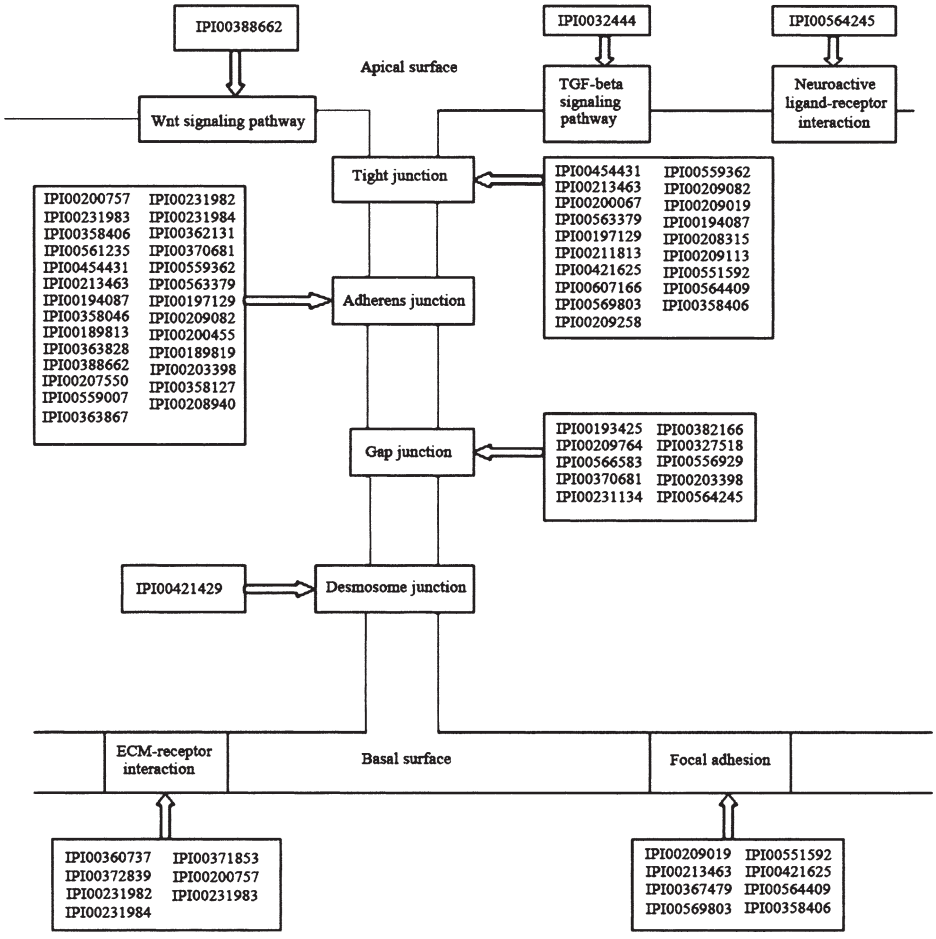

Figure 8. Proteins involved in the cell communication pathway. The IPI accession numbers of proteins are displayed in the related rectangle linked to their functions through arrows.

form a network from cadherin and β-catenin to α-catenin. Furthermore, ten known gap junction proteins, seven extracellular matrix-receptor interaction proteins and eight focal adhesion proteins were also identified. Comparing the proteins from different fractions, we found that most of them were from the microdomain fractions. The results further indicate that the microdomain strategy is a good method for the enrichment and identification of low-abundance membrane proteins.

Conclusions. Highly purified PM was enriched by twofold sucrose density centrifugation. Many low-abundant integral membrane proteins were enriched and identified by the three different strategies, especially the microdomain fractionation strategy. To our knowledge, this is the first systematic proteome analysis of microdomain fractions in rat liver PM. This strategy can help us to develop global proteomic analysis of the proteins residing within these very important functional substructures of PM-caveolae and lipid rafts. Through the enrichment of microdomain fractions, we not only identified many high-abundance proteins such as sodium/potassium-transporting ATPase α-1 chain precursor, 5′-nucleotidase precursor, ADP, ATP carrier protein 2 and so on, which have been found in similar microdomain proteomic analyses, but also many low-abundance proteins. For example, 42 caveolae-specific proteins, obtained through subtraction proteomic analysis, were found, and most of these had not been found in caveolae- and lipid-raft-enriched proteomic analysis [8, 10, 42]. Furthermore, in all identified 457 non-redundant proteins, 46% came from microdomain fractions. Not only the higher-molecular-weight proteins but also higher TM proteins were obtained in the microdomain fractionation strategy compared with Na_2CO_3 treatment and C/M extraction. This may be because the microdomain strategy enhances detection of low-abundance proteins. Among all the identified proteins, 42% were PM or PM-associated proteins, and 33% had no assigned location. About 10% of the proteins were proteins involved in the cell communication pathway. These results suggested that our hydrophobic membrane enrichment and microdomain strategies facilitate proteomic analysis of hydrophobic and low-abundance proteins. Our results also showed that membrane proteomics will allow for more

comprehensive characterization and will enable a better understanding of membrane protein dynamics in the future. Furthermore, the analysis of microdomain fractions revealed fine details of the complex protein architecture at the rat liver PM. This overall view of the microdomains that we offer here will hopefully stimulate interest in future functional studies.

Acknowledgements. This work was supported by a grant from National 973 Project of China (2001 CB5102), a grant from CHLPP (2004 BA711A11), National Natural Science Foundation of China (30000028, 30240056), and a project of PCSIRT (IRT0445).

1 Brunet, S., Thibault, P., Gagnon, E., Kearney, P., Bergeron, J. J. and Desjardins, M. (2003) Organelle proteomics: looking at less to see more. Trends Cell Biol. 13, 629–638.
2 Adam, P. J., Boyd, R., Tyson, K. L., Fletcher, G. C., Stamps, A., Hudson, L., Poyser, H. R., Redpath, N., Griffiths, M., Steers, G., Harris, A. L., Patel, S., Berry, J., Loader, J. A., Townsend, R. R., Daviet, L., Legrain, P., Parekh, R. and Terrett, J. A. (2003) Comprehensive proteomic analysis of breast cancer cell membranes reveals unique proteins with potential roles in clinical cancer. J. Biol. Chem. 278, 6482–6489.
3 Oh, P., Li, Y., Yu, J., Durr, E., Krasinska, K. M., Carver, L. A., Testa, J. E. and Schnitzer, J. E. (2004) Subtractive proteomic mapping of the endothelial surface in lung and solid tumours for tissue-specific therapy. Nature. 429, 629–635.
4 Stevens, S. M. Jr, Zharikova, A. D. and Prokai, L. (2003) Proteomic analysis of the synaptic plasma membrane fraction isolated from rat forebrain. Brain Res. Mol. Brain Res. 117, 116–128.
5 Gottesman, M. M., Fojo, T. and Bates, S. E. (2002) Multidrug resistance in cancer: role of ATP-dependent transporters. Nat. Rev. Cancer 2, 48–58.
6 Goette, A., Lendeckel, U. and Klein, H. U. (2002) Signal transduction systems and atrial fibrillation. Cardiovasc. Res. 54, 247–258.
7 Paulsen, I. T., Sliwinski, M. K., Nelissen, B., Goffeau, A. and Saier, M. H. Jr (1998) Unified inventory of established and putative transporters encoded within the complete genome of *Saccharomyces cerevisiae*. FEBS Lett. 430, 116–125.
8 Raimondo, F., Ceppi, P., Guidi, K., Masserini, M., Foletti, C. and Pitto, M. (2005) Proteomics of plasma membrane microdomains. Expert Rev. Proteom. 2, 793–807.
9 Lisanti, M. P., Scherer, P. E., Vidugiriene, J., Tang, Z., Hermanowski-Vosatka, A., Tu, Y. H., Cook, R. F. and Sargiacomo, M. (1994) Characterization of caveolin-rich membrane domains isolated from an endothelial-rich source: implications for human disease. J. Cell Biol. 126, 111–126.
10 Sprenger, R. R., Speijer, D., Back, J. W., De Koster, C. G., Pannekoek, H. and Horrevoets, A. J. (2004) Comparative proteomics of human endothelial cell caveolae and rafts using two-dimensional gel electrophoresis and mass spectrometry. Electrophoresis 25, 156–172.
11 Zhang, L., Xie, J., Wang, X., Liu, X., Tang, X., Cao, R., Hu, W., Nie, S., Fan, C. and Liang, S. (2005) Proteomic analysis of mouse liver plasma membrane: use of differential extraction to enrich hydrophobic membrane proteins. Proteomics 5, 4510–4524.
12 Henningsen, R., Gale, B. L., Straub, K. M. and DeNagel, D. C. (2002) Application of zwitterionic detergents to the solubilization of integral membrane proteins for two-dimensional gel electrophoresis and mass spectrometry. Proteomics 2, 1479–1488.
13 Santoni, V., Kieffer, S., Desclaux, D., Masson, F. and Rabilloud, T. (2000) Membrane proteomics: use of additive main effects with multiplicative interaction model to classify plasma membrane proteins according to their solubility and electrophoretic properties. Electrophoresis 21, 3329–3344.
14 Zhang, L., Liu, X., Zhang, J., Cao, R., Lin, Y., Xie, J., Chen, P., Sun, Y., Li, D. and Liang, S. (2006) Proteome analysis of combined effects of androgen and estrogen on the mouse mammary gland. Proteomics 6, 487–497.
15 Zhang, L., Liu, X., Zhang, J., Cao, R., Lin, Y., Xie, J., Chen, P., Sun, Y., Li, D. and Liang, S. (2006) Proteome analysis of combined effects of androgen and estrogen on the mouse mammary gland. Proteomics 6 (2), 487–497.
16 Gobom, J., Schuerenberg, M., Mueller, M., Theiss, D., Lehrach, H. and Nordhoff, E. (2001) Alpha-cyano-4-hydroxycinnamic acid affinity sample preparation: a protocol for MALDI-MS peptide analysis in proteomics. Anal. Chem. 73, 434–438.
17 Maurer, M. H., Feldmann, R. E. Jr, Futterer, C. D. and Kuschinsky, W. (2003) The proteome of neural stem cells from adult rat hippocampus. Proteom. Sci. 1, 4.
18 Cao, R., Li, X., Liu, Z., Peng, X., Hu, W., Wang, X., Chen, P., Xie, J. and Liang, S. (2006) Integration of a two-phase partition method into proteomics research on rat liver plasma membrane proteins. J. Proteom. Res. 5, 634–642.
19 Perkins, D. N., Pappin, D. J., Creasy, D. M. and Cottrell, J. S. (1999) Probability-based protein identification by searching sequence databases using mass spectrometry data. Electrophoresis 20, 3551–3567.
20 Liu, H., Sadygov, R. G. and Yates, J. R., 3rd (2004) A model for random sampling and estimation of relative protein abundance in shotgun proteomics. Anal. Chem. 76, 4193–4201.
21 Kyte, J. and Doolittle, R. F. (1982) A simple method for displaying the hydropathic character of a protein. J. Mol. Biol. 157, 105–132.
22 Ashburner, M., Ball, C. A., Blake, J. A., Botstein, D., Butler, H., Cherry, J. M., Davis, A. P., Dolinski, K., Dwight, S. S., Eppig, J. T., Harris, M. A., Hill, D. P., Issel-Tarver, L., Kasarskis, A., Lewis, S., Matese, J. C., Richardson, J. E., Ringwald, M., Rubin, G. M. and Sherlock, G. (2000) Gene ontology: tool for the unification of biology. The Gene Ontology Consortium Nat. Genet. 25, 25–29.
23 Melen, K., Krogh, A. and von Heijne, G. (2003) Reliability measures for membrane protein topology prediction algorithms. J. Mol. Biol. 327, 735–744.
24 Molloy, M. P., Herbert, B. R., Walsh, B. J., Tyler, M. I., Traini, M., Sanchez, J. C., Hochstrasser, D. F., Williams, K. L. and Gooley, A. A. (1998) Extraction of membrane proteins by differential solubilization for separation using two-dimensional gel electrophoresis. Electrophoresis 19, 837–844.
25 Marmagne, A., Rouet, M. A., Ferro, M., Rolland, N., Alcon, C., Joyard, J., Garin, J., Barbier-Brygoo, H. and Ephritikhine, G. (2004) Identification of new intrinsic proteins in *Arabidopsis* plasma membrane proteome. Mol. Cell Proteom. 3, 675–691.
26 Ferro, M., Salvi, D., Riviere-Rolland, H., Vermat, T., Seigneurin-Berny, D., Grunwald, D., Garin, J., Joyard, J. and Rolland, N. (2002) Integral membrane proteins of the chloroplast envelope: identification and subcellular localization of new transporters. Proc. Natl. Acad. Sci. USA 99, 11487–11492.
27 Ferro, M., Seigneurin-Berny, D., Rolland, N., Chapel, A., Salvi, D., Garin, J. and Joyard, J. (2000) Organic solvent extraction as a versatile procedure to identify hydrophobic chloroplast membrane proteins. Electrophoresis 21, 3517–3526.
28 Link, A. J., Eng, J., Schieltz, D. M., Carmack, E., Mize, G. J., Morris, D. R., Garvik, B. M. and Yates, J. R., 3rd (1999) Direct analysis of protein complexes using mass spectrometry. Nat. Biotechnol. 17, 676–682.
29 Peng, J., Elias, J. E., Thoreen, C. C., Licklider, L. J. and Gygi, S. P. (2003) Evaluation of multidimensional chromatography coupled with tandem mass spectrometry (LC/LC-MS/MS) for large-scale protein analysis: the yeast proteome. J. Proteom. Res. 2, 43–50.
30 Schagger, H. and von Jagow, G. (1987) Tricine-sodium dodecyl sulfate-polyacrylamide gel electrophoresis for the separation of

proteins in the range from 1 to 100 kDa. Anal. Biochem. 166, 368–379.
31 Zhang, L., Xie, J., Wang, X., Liu, X., Tang, X., Cao, R., Hu, W., Nie, S., Fan, C. and Liang, S. (2005) Proteomic analysis of mouse liver plasma membrane: use of differential extraction to enrich hydrophobic membrane proteins. Proteomics 5 (17), 4510–4524.
32 Fountoulakis, M. and Suter, L. (2002) Proteomic analysis of the rat liver. J. Chromatogr. B Anal. Technol. Biomed. Life Sci. 782, 197–218.
33 Fountoulakis, M. and Takacs, B. (2001) Effect of strong detergents and chaotropes on the detection of proteins in two-dimensional gels. Electrophoresis 22, 1593–1602.
34 Cutillas, P. R., Biber, J., Marks, J., Jacob, R., Stieger, B., Cramer, R., Waterfield, M., Burlingame, A. L. and Unwin, R. J. (2005) Proteomic analysis of plasma membrane vesicles isolated from the rat renal cortex. Proteomics 5, 101–112.
35 Zhao, Y., Zhang, W., Kho, Y. and Zhao, Y. (2004) Proteomic analysis of integral plasma membrane proteins. Anal. Chem. 76, 1817–1823.
36 Alexandersson, E., Saalbach, G., Larsson, C. and Kjellbom, P. (2004) *Arabidopsis* plasma membrane proteomics identifies components of transport, signal transduction and membrane trafficking. Plant Cell Physiol. 45, 1543–1556.
37 Moller, S., Mix, E., Bluggel, M., Serrano-Fernandez, P., Koczan, D., Kotsikoris, V., Kunz, M., Watson, M., Pahnke, J., Illges, H., Kreutzer, M., Mikkat, S., Thiesen, H. J., Glocker, M. O., Zettl, U. K. and Ibrahim, S. M. (2005) Collection of soluble variants of membrane proteins for transcriptomics and proteomics. In Silico Biol. 5, 295–311.
38 Khan, I. U., Wallin, R., Gupta, R. S. and Kammer, G. M. (1998) Protein kinase A-catalyzed phosphorylation of heat shock protein 60 chaperone regulates its attachment to histone 2B in the T lymphocyte plasma membrane. Proc. Natl. Acad. Sci. USA 95, 10425–10430.
39 Hariton-Gazal, E., Rosenbluh, J., Graessmann, A., Gilon, C. and Loyter, A. (2003) Direct translocation of histone molecules across cell membranes. J. Cell Sci. 116, 4577–4586.
40 Jiang, X. S., Dai, J., Sheng, Q. H., Zhang, L., Xia, Q. C., Wu, J. R. and Zeng, R. (2005) A comparative proteomic strategy for subcellular proteome research: ICAT approach coupled with bioinformatics prediction to ascertain rat liver mitochondrial proteins and indication of mitochondrial localization for catalase. Mol. Cell Proteom. 4, 12–34.
41 Hentula, M., Peltonen, J. and Peltonen, S. (2001) Expression profiles of cell-cell and cell-matrix junction proteins in developing human epidermis. Arch. Dermatol. Res. 293, 259–267.
42 Foster, L. J., De Hoog, C. L. and Mann, M. (2003) Unbiased quantitative proteomics of lipid rafts reveals high specificity for signaling factors. Proc. Natl. Acad. Sci. USA 100, 5813–5818.